An Extensive Car-Following Model With Driver Memory

Priyanka
Department of Mathematics
Government College, Meham
Rohtak, India
priyankasiwach199@gmail.com

Poonam Redhu
Department of Mathematics
Maharshi Dayanand University
Rohtak, India
poonamr.maths@mdurohtak.ac.in

ABSTRACT

In this chapter, we present an expanded car-following model that takes into account the collective influence of the driver's sensory memory as well as the velocity differential between the following and leading vehicles in the traffic flow process. The stability conditions are determined by doing a linear stability analysis on three types of traffic flows in the headway-sensitivity space: stable, metastable, and unstable. Furthermore, numerical simulation of the space-time evolution of headways and headway profiles is performed. The numerical simulation results match closely with the theoretical conclusions. The following car driver's sensory buffer time and velocity differential play a crucial influence on traffic flow stability, according to both analytical and simulation data.

Keywords— Car-following, Stability analysis, Driver's memory

I. INTRODUCTION

In the last 60 years, the idea of the development of various theories related to traffic flow has come into existence. On the basis of different approaches and mathematical methods, researchers have given very satisfactory consequences in the field of traffic theory. The most common and serious problem with traffic dynamics is traffic jams. Because of the tremendous quantitative increase in vehicles, traffic congestion has become a major transportation issue. To handle these types of challenges, researchers have developed a wide range of traffic flow models and theories. These traffic flow models are significant for the improvement of precise tools for understanding, simulating, and controlling urban transportation systems.

In this chapter, we are concerned with the microscopic approach. As a basic and important component of the microscopic approach, car-following theory has been theoretically studied. The car-following theory represents and illustrates the relationship between the leading and following vehicles. In the last few decades, many car-following models like the "optimal velocity model by Bando et al. [1], full velocity difference model by Jiang et al. [2], generalized

force model by Helbing and Tilch [3], GM model [4] etc. have been developed. In addition, many extended car-following models have been proposed to analyze various real factors of traffic flow such as the honk effect [5, 6], ITS environment [8, 9], cooperative driving systems [10], driver's anticipation [11] and heterogeneous vehicles [12] etc."

However, the preceding traffic flow models do not take into account the driver's memory effect. In this direction, Zhang [13] presented a "macro model" by taking the driver's memory impact into account, Peng et al. [14] presented a "driver's memory lattice model," and it is observed that the memory of past information plays a significant role in the driving process of a driver and presented a car-following model by taking the driver's memory effect into account. The above-discussed models consider the memory only at earlier time t-τ_0, but avoid the traffic states between [t-τ_0, t].

Later, Cao [15] developed a car-following model by considering the driver's sensory memory (Mean Memory Model) over a period of time [t-τ_0, t] and observed that the developed model is more realistic. However, the impact of velocity difference is not considered in this model. Actually, the velocity difference may have a significant impact on the traffic flow. The velocity difference effect, not only improved the traffic flow stability but also resolved the problems of collision and improbable deceleration.

In this chapter, we extended the main memory model by incorporating the effect of velocity difference and presented a new traffic flow model named as "an extended car-following model considering driver's memory and velocity difference".

The chapter is laid out as follows: in section II, we gave the model equation. In Section III, we examined the suggested model's linear stability. Section IV employs numerical simulation to validate theoretical findings. The conclusion comes in Section V. The findings of the linear stability investigation and numerical simulation reveal that the current model is more realistic than previous models.

II. NEW MODEL

In this chapter, we proposed a new car-following model by introducing velocity difference term into the mean memory model [15]. The main equation of this model is given below

$$\frac{dv_j}{dt} = \alpha[V\{\Delta x_j(t\text{-}\tau_1) - v_j\}] + k\,\Delta v_j(t) \quad (1)$$

where v_j represent the velocity of j^{th} car at time t, $\alpha = \frac{1}{\tau}$ is the "sensitivity coefficient" of a driver, $\Delta x_j(t\text{-}\tau_1)$ represents the mean headway in the interval [t-τ_0,t] and τ_0 is the driver sensory memory time. The term

$\Delta v_j(t) = v_{j+1}(t) - v_j(t)$

represents the velocity difference of $j+1^{th}$ and j^{th} vehicle at time t, k = $\frac{\lambda}{\tau}$ is the reaction coefficient of response for velocity difference $\Delta v_j(t)$ and V represents "optimal velocity function".

Equation (1) displays that acceleration of j^{th} car at time t is calculated by the optimal velocity, which depends on mean headway, velocity of j^{th} car and velocity difference of preceding car $j+1^{th}$ and the following car j^{th} at time t.

Now, expanding the term $\Delta x_j(t-\tau_1)$ in equation (1) by Taylor series about τ_1, we obtain

$$\Delta x_j(t-\tau_1) = \Delta x_j(t) - \tau_1 \frac{d\Delta x_j(t)}{dt} + o(\tau_1) \quad (2)$$

where $o(\tau_1)$ represents the terms containing higher power of τ_1. By neglecting the terms containing higher power in equation (2) and then using in equation (1), we get

$$\frac{dv_j}{dt} = \alpha[V\{\Delta x_j(t)\} - \tau_1 \frac{d\Delta x_j(t)}{dt}\} - v_j(t)] + k\Delta v_j(t)$$

$$\frac{dv_j}{dt} = \alpha[V\{\Delta x_j(t)\} - \tau_1 \Delta v_j(t)\} - v_j(t)] + k[v_{j+1}(t) - v_j(t)] \quad (3)$$

Again by Taylor series expansion of $V\{\Delta x_j(t)\} - \tau_1 \Delta v_j(t)\}$ about $\tau_1 \Delta v_j(t)$ and ignoring the non-linear terms, we obtained

$$V\{\Delta x_j(t)\} - \tau_1 \Delta v_j(t)\} = V\{\Delta x_j(t)\} - \tau_1 \Delta v_j(t) V'((\Delta x(t)_j) \quad (4)$$

where $V'((\Delta x(t)_j)$ denotes the derivative of optimal velocity function w.r.t. headway at time t.

Using equation (4) into (3), we have

$$\frac{dv_j}{dt} = \alpha[V\{\Delta x_j(t)\} - \tau_1 \Delta v_j(t) V'((\Delta x(t)_j) - v_j(t)] + k[v_{j+1}(t) - v_j(t)] \quad (5)$$

If $\tau_1 = 0$ and $\lambda = 0$, then given model becomes optimal velocity model.

For model stability analysis, we describe the equation (5) using finite difference method, we have

$$v_j(t+\tau) = v_j(t) + \alpha\tau[V\{\Delta x_j(t)\} - \tau_1\{v_{j+1}(t) - v_j(j)\}V'\left(\Delta x_j(t)\right) - v_j(t)] + k[v_{j+1}(t) - v_j(t)]$$

$$v_j(t+\tau) = [V\{\Delta x_j(t)\} - \tau_1\{v_{j+1}(t) - v_j(j)\}V'(\Delta x_j(t))] + \lambda[v_{j+1}(t) - v_j(t)] \quad (6)$$

Again using finite difference method in equation (6), we get

$$x_j(t+2\tau) = x_j(t+\tau) + \tau\, V\{\Delta x_j(t)\} - \tau_1[\Delta x_j(t+\tau) - \Delta x_j(t)]\, V'(\Delta x_j(t) + \lambda[\Delta x_j(t+\tau) - \Delta x_j(t)] \quad (7)$$

The following optimal velocity function is used in this model:

$$V(\Delta x_j) = V_1 + V_2[\tanh C_1(\Delta x_j - l_c) - C_2] \quad (8)$$

where l_c is the car's length. The above formula is used in many car- following models.

III. LINEAR STABILITY ANALYSIS

The suggested model is not subjected to linear analysis in this part. To begin, we assume traffic flow stability in terms of uniform flow. Uniform traffic flow is defined as all vehicles travelling with the same headway 'h', the optimal velocity V(h), and the relative velocity is set to zero. Clearly, the consistently steady-state solution of equation (5) can be represented as

$$x_j^0 = hj + V(h)t \quad (9)$$

where h denotes the steady-state headway and h =L/N, L is road length, N is the entire number of vehicles, V(h) is the optimal velocity in uniform traffic flow and $x_j^0(t)$ represent the location of the vehicle in steady-state.

Let $y_j(t)$ be a small perturbation from the uniform steady state solution $x_j^0(t)$, i.e.,

$$x_j(t) = x_j^0(t) + y_j(t) \quad (10)$$

and the corresponding headway is

$$\Delta x_j(t) = h + \Delta y_j(t) \quad (11)$$

Using equations (10) and (11) into equation (8), we obtain

$y_j''(t) = \alpha[V\{h + \Delta y_j(t)\} - \tau_1 \Delta y_j'(t) V'\{h + \Delta y_j(t)\} - \{V(h) + y_j'(t)\}] + k\Delta y_j'(t)$

Expanding the terms $V\{h + \Delta y_j(t)\}$ & $V'\{h + \Delta y_j(t)$ by taylor series and neglecting the higher power of $\Delta y_j(t)$, then we get the following linear equation:

$$y_j''(t) = \alpha[\Delta y_j(t) V'(h) - \tau_1 \Delta y_j'(t)\, V'(h) - y_j'(t)] + k\Delta y_j'(t) \quad (12)$$

where $y_j''(t)$ represents the second order derivative w.r.t. 't', $\Delta y_j(t) = y_{j+1}(t) - y_j(t)$ and $V'(h) = [\frac{d\Delta V(\Delta x)}{d\Delta x}]_{\Delta x = h}$.

Expanding $y_j(t) = Be^{(ikj+zt)}$(Fourier modes) and let $\tau_1 = p\tau$, p is a parameter, we have

$$z^2 + [(e^{ik} - 1)(pV'(h) - k) + \alpha]z - \alpha(e^{ik} - 1)\, V'(h) = 0 \quad (13)$$

By expanding $z = z_1(ik) + z_2(ik)^2 \ldots$, substituting this value of z into equation (13) and ignoring the higher order terms, we get

$$[z_1(ik) + z_2(ik)^2]^2 + [\{(ik) + \tfrac{(ik)^2}{2}\}(pV'(h) - k) + \alpha]^* \\ (z_1(ik) + z_2(ik)^2) - \alpha\{(ik) + \tfrac{(ik)^2}{2}\}\, V'(h) = 0$$

Comparing the coefficients of (ik) and $(ik)^2$ on both sides, we get

$$\begin{cases} z_1 = V'(h) \\ z_2 = \dfrac{V'(h)}{2\alpha}[(1+2\lambda)\alpha - 2pV'(h)] - \dfrac{(V'(h))^2}{\alpha} \end{cases} \quad (14)$$

For small disturbance of long wavelength, the uniform traffic flow is unstable if $z_2 < 0$, while uniform flow is stable if $z_2 > 0$.

Therefore, "the neutral stability condition" is given by putting $z_2 = 0$. i.e.,

$$\frac{V'(h)}{2}[(1+2\lambda)\alpha - 2pV'(h)] - (V'(h))^2 = 0$$

$$V'(h) = \frac{(1+2\lambda)\alpha}{2(1+p)} \quad (15)$$

Consequently, the uniform traffic flow is stable for long wavelength if,

$$V'(h) < \frac{(1+2\lambda)\alpha}{2(1+p)} \quad (16)$$

The neutral stability curves are shown in figures 1(a), 1(b) and 1(c) with the help of stability condition (16) in the parameter space $(\Delta x, \alpha)$.

From the figures, it is clear that there exist different critical points (h_c, α_c) for the neutral stability curves for distinct sets of (λ, p). The peaks of each curve show the critical point. If $\alpha > \alpha_c$, the uniform steady state is always linearly stable irrespective of vehicle headway and if $\alpha < \alpha_c$, the uniform steady state in neighbourhood of h_c is unstable.

The neutral stability curves divide the region into two sub-regions (a) stable (b) unstable. Traffic flow is stable above the neutral stability curves but unstable below the neutral stability curves. Therefore, traffic jams will not appear in the stable region which we will also prove in the simulation result.

It can be easily from the fig. 1(a) that the increasing the value of sensory memory coefficient p, the amplitude of neutral stability curves increases i.e., the stable region decreases with increasing the value of p. Similar results hold for $\lambda = 0.3$ and $\lambda = 0.5$ as shown in fig. 1(b) and fig. 1(c), respectively.

From figures 1(a), 1(b) and 1(c), it is found that for a particular value of 'p' the amplitude as well as critical sensitivity decrease with an increase in the value of λ i.e., stable area improves with an increase in the value of λ. Therefore, we can conclude that velocity difference plays an important role in reducing the traffic congestion.

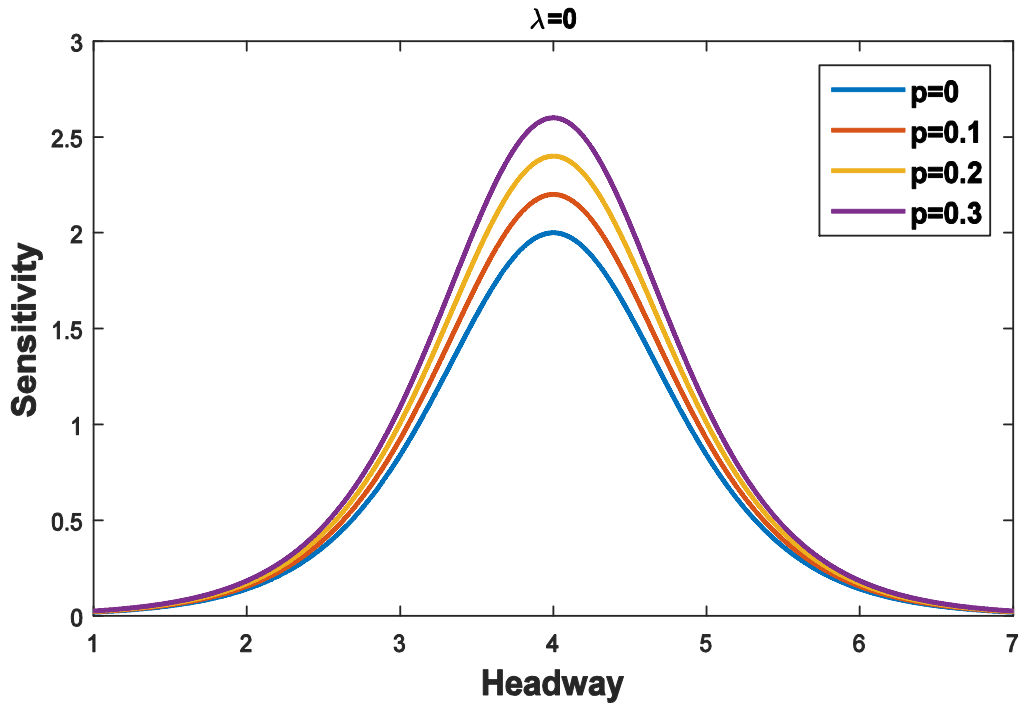

Fig. 1(a): "Neutral Stability Curve in the Headway-Sensitivity Space for λ = 0 and different Values of p"

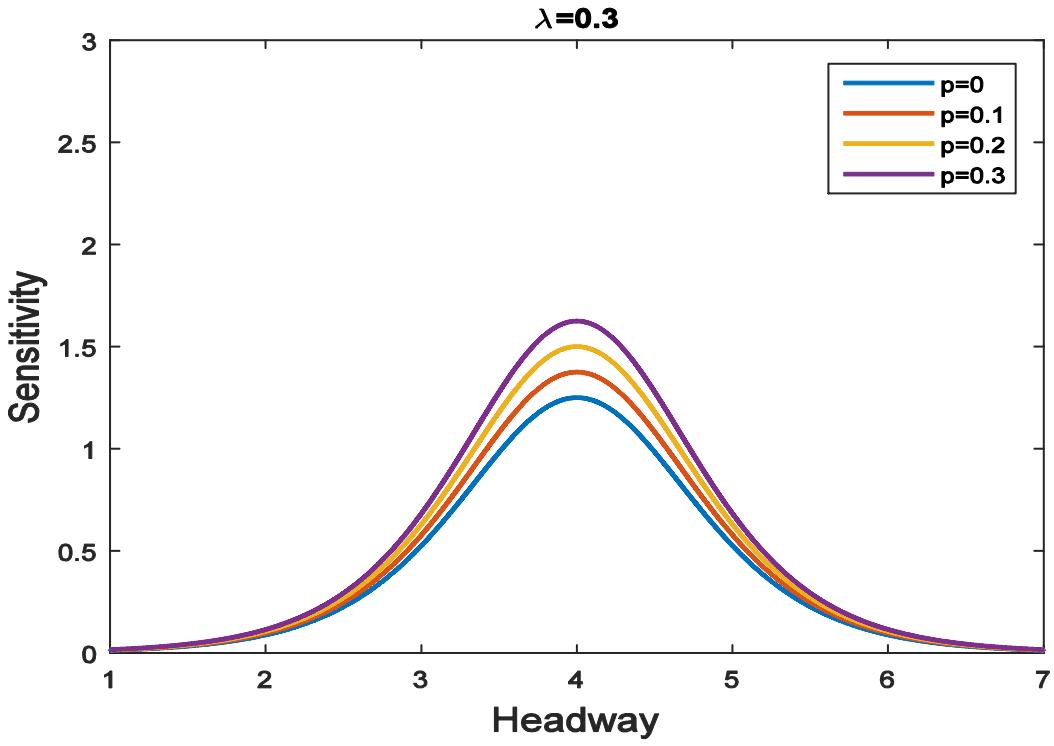

Fig. 1(b): "Neutral stability curves in the headway-sensitivity space for λ = 0.3 and different values of p"

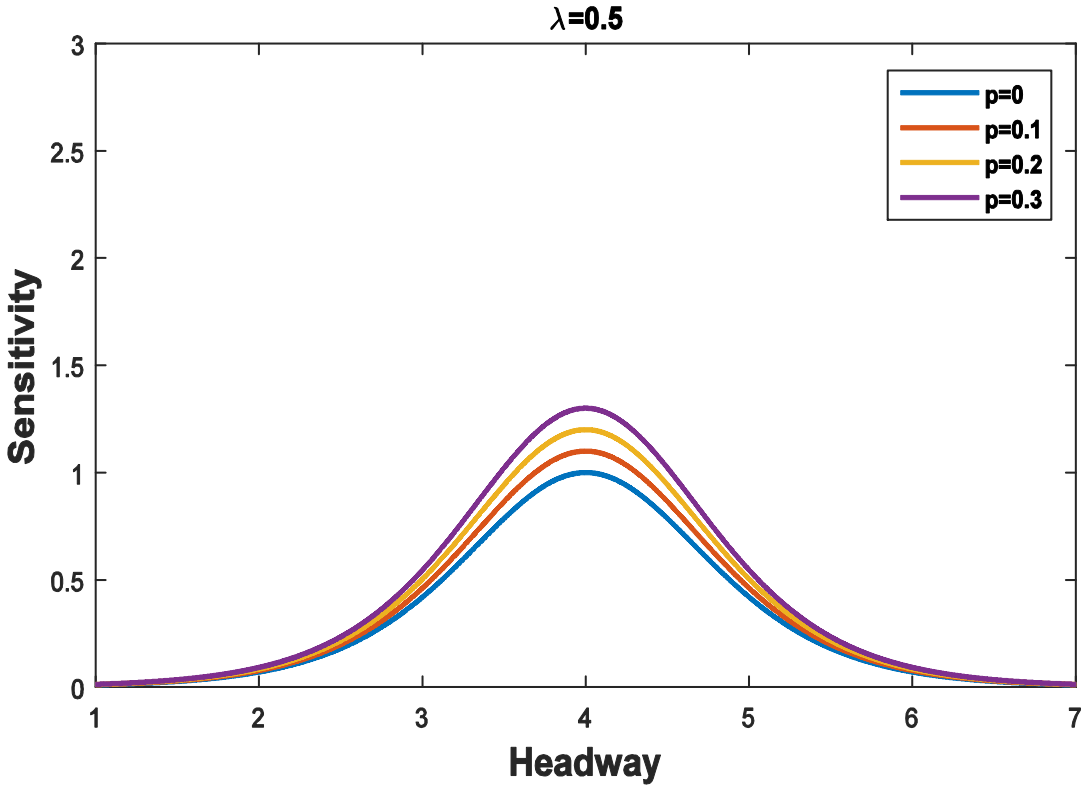

Fig. 1(c): "Neutral stability curve in the headway-sensitivity space for λ = 0.5 and different values of p"

IV. NUMERICAL SIMULATION

The suggested study is numerically simulated to investigate the effect of driver memory and velocity difference on "spatial-time evolution of headway" and "headway profile" when a tiny disturbance appears. In order to simulate the current model, we rewrite equation (7) in terms of headway as follows:

$$\begin{aligned}\Delta x_j(t+2\tau) = \Delta x_j(t+\tau) + \tau\left[V\left(\Delta x_{j+1}(t)\right) - V\left(\Delta x_j(t)\right)\right] \\ - p\tau\left[\Delta x_{j+2}(t+\tau) - \Delta x_{j+1}(t+\tau) - \Delta x_{j+2}(t) + \Delta x_{j+1}(t) - \Delta x_{j+1}(t+\tau)\right. \\ \left. + \Delta x_j(t+\tau) + \Delta x_{j+1}(t) - \Delta x_j(t)\right]\left[V'\left(\Delta x_{j+1}(t)\right) - V'\left(\Delta x_j(t)\right)\right] \\ + \lambda[\Delta x_{j+2}(t+\tau) - \Delta x_{j+1}(t+\tau) - \Delta x_{j+2}(t) + \Delta x_{j+1}(t) - \Delta x_{j+1}(t+\tau) \\ + \Delta x_j(t+\tau) + \Delta x_{j+1}(t) - \Delta x_j(t)]\end{aligned}$$

Simulation is performed under periodic boundary condition. Initially, assume that there are J = 100 vehicles are uniformly distributed on a road of length(L) = 1500m. The initial conditions are chosen as follows:

$\Delta x_j(t)|_{t=0} = \Delta x_j(t)|_{t=1} = \Delta x_0 = \frac{L}{J}$, j = 1,2,3,…,100

$\Delta x_j(t)|_{t=2} = \Delta x_0 = \frac{L}{J}, \quad j \neq 1, j \neq 2$

$\Delta x_j(t)|_{t=2} = \Delta x_0 + 0.5, \quad j = 1$

$\Delta x_j(t)|_{t=2} = \Delta x_0 - 0.5, \quad j = 2$

Other input parameters are as follows:

$V_{max} = V(L/J), \ \alpha = \frac{1}{\tau} = 2s^{-1}$

where J = 100 and L = 1500m.

Figures 2(a)-2(d) represent the "spatiotemporal evolution of the headway" after t = 10000s for distinct values of p when λ = 0. From the figures 2(b)-2(d), it can be easily seen that the initial uniform perturbation converts into "kink-antikink density wave" which are the solution of mKdV equation. These density waves propagate over time in the opposite direction as shown in figure and these observations are same as that happen in real traffic. As we enter into stable region for p = 0, these traffic wave evolves straight line.

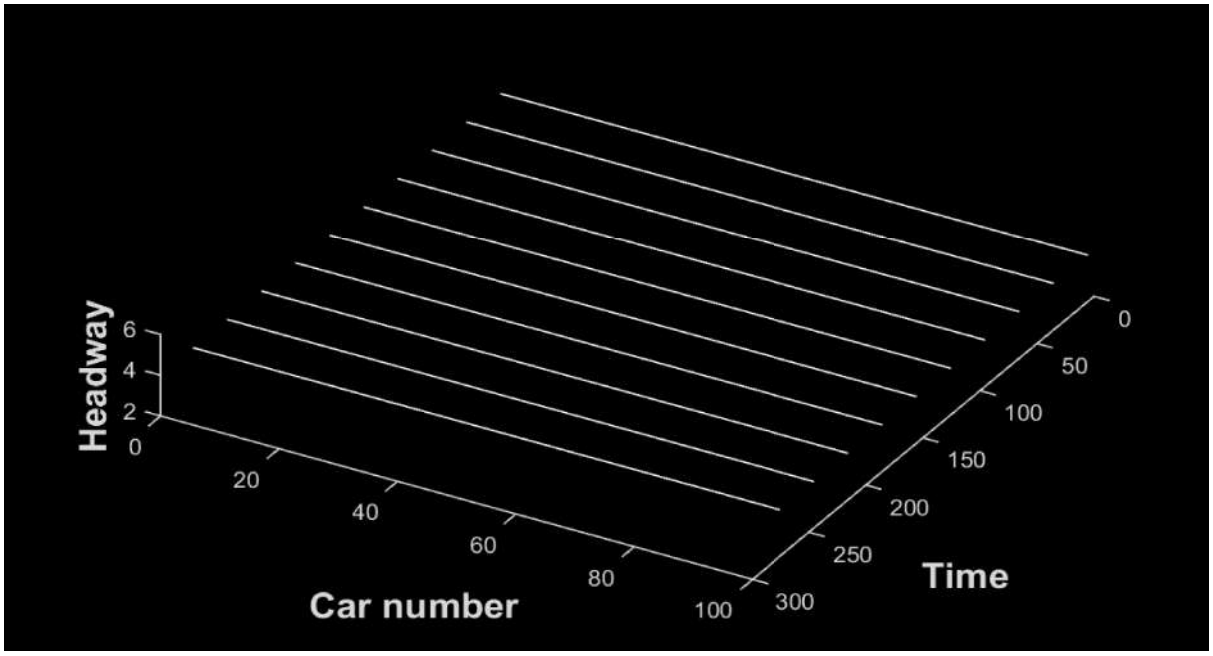

Fig. 2(a): "Headway evolution in space and time after t = 10000s for λ = 0 and p = 0"

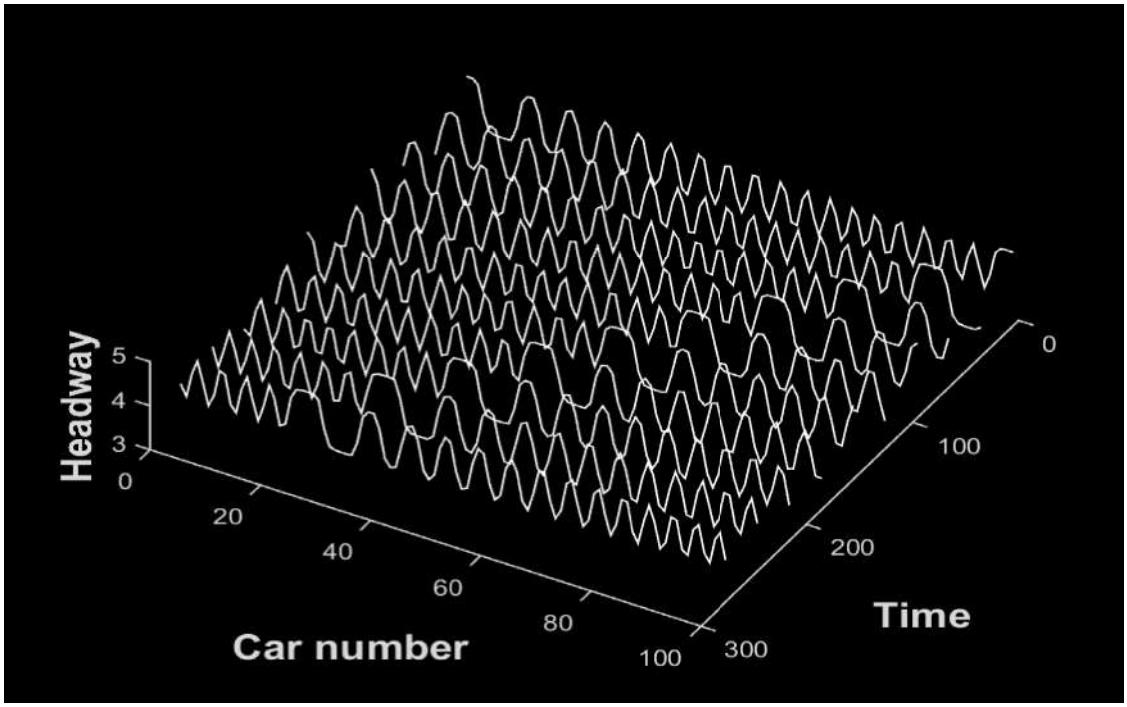

Fig. 2(b): "Headway evolution in space and time after t = 10000s for λ = 0 and p = 0.1"

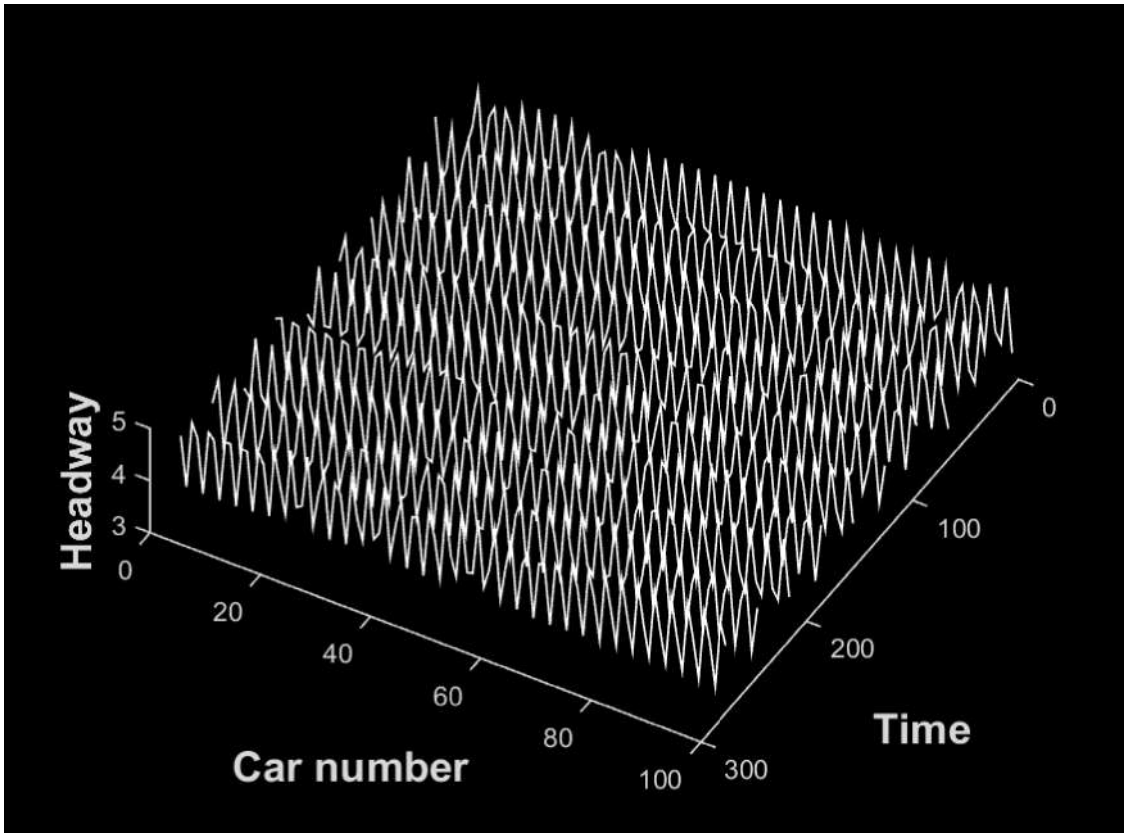

Fig. 2(c): "Headway evolution in space and time after t = 10000s for λ = 0 and p = 0.2"

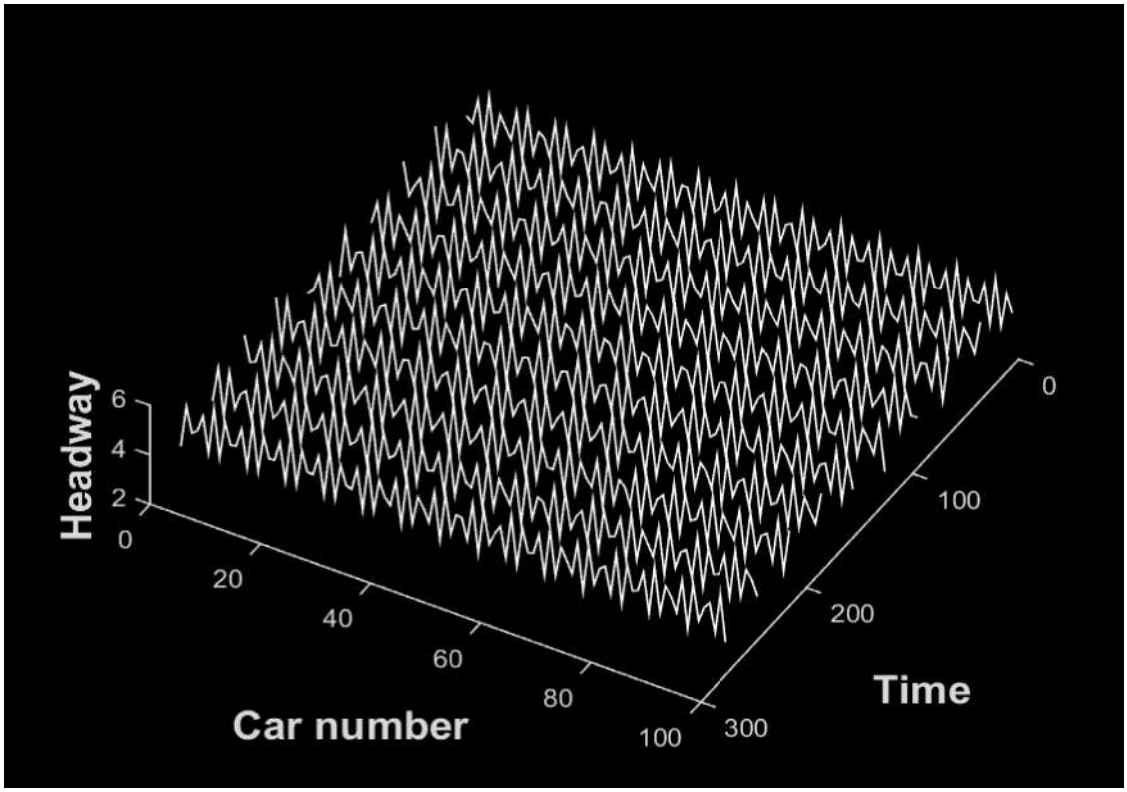

Fig. 2(d): "Headway evolution in space and time after t = 10000s for λ = 0 and p = 0.3"

Figures 3(a)-3(d) represent the graph between headway profile after t = 10000s for different values of p when $\lambda = 0$. Figure 3(a) shows that density wave dies out and the kink- antikink waves convert into a single line which represents that there is no traffic congestion.

Further from figures 3(b), 3(c) and 3(d), we can observe that the amplitude of density waves rises with an increase in the value of p which shows that the region of traffic congestion growths with increase in the value of p.

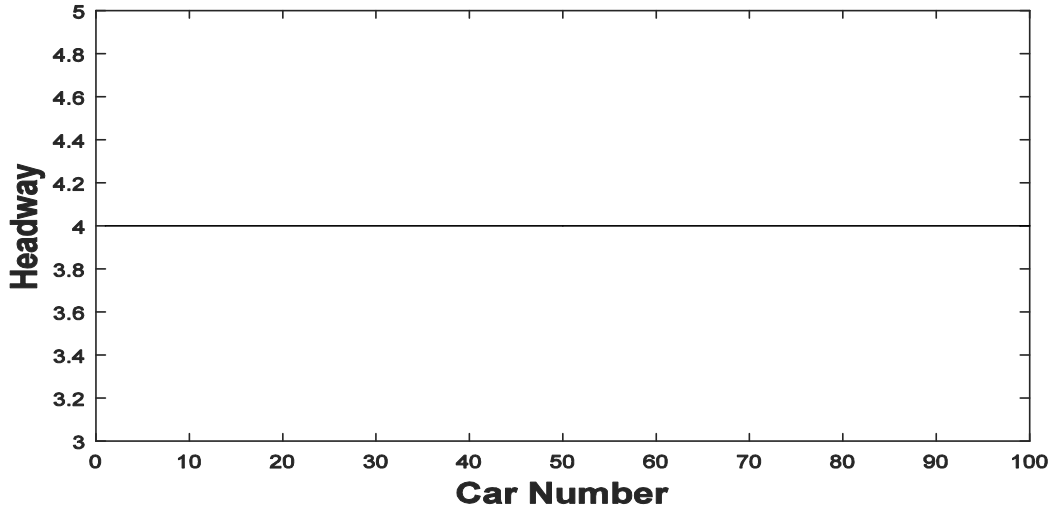

Fig. 3 (a): "Headway profiles at t = 10000s, the figure corresponding to λ = 0 and p = 0"

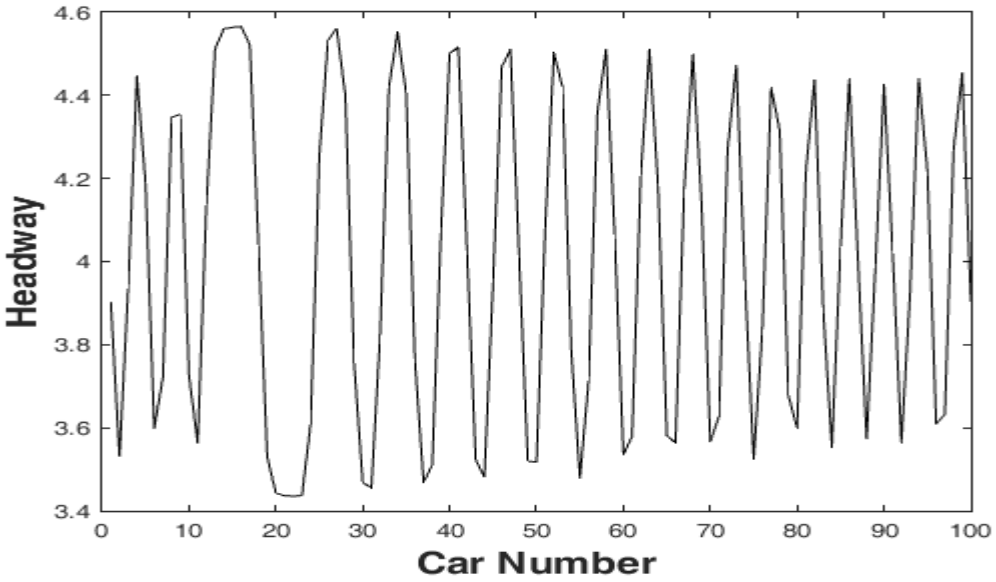

Fig. 3(b): " Headway profiles at t =10000s, the figure corresponding to $\lambda = 0$ and $p = 0.1$"

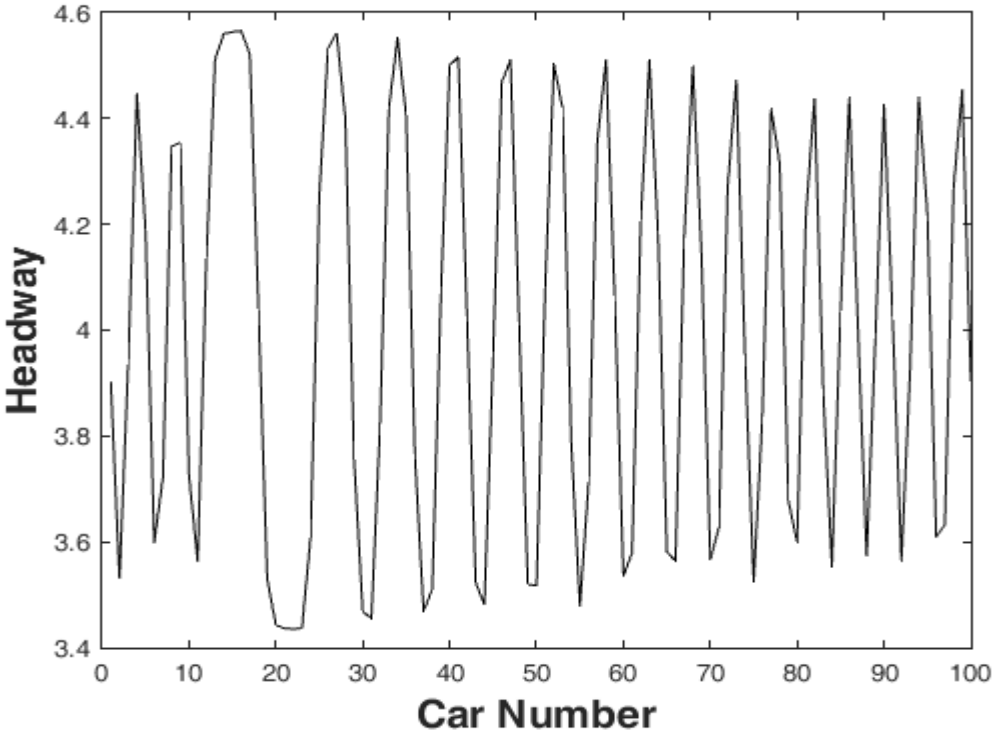

Fig. 3(c): "Headway profiles at t =10000s, the figure corresponding to $\lambda = 0$ and $p = 0.2$"

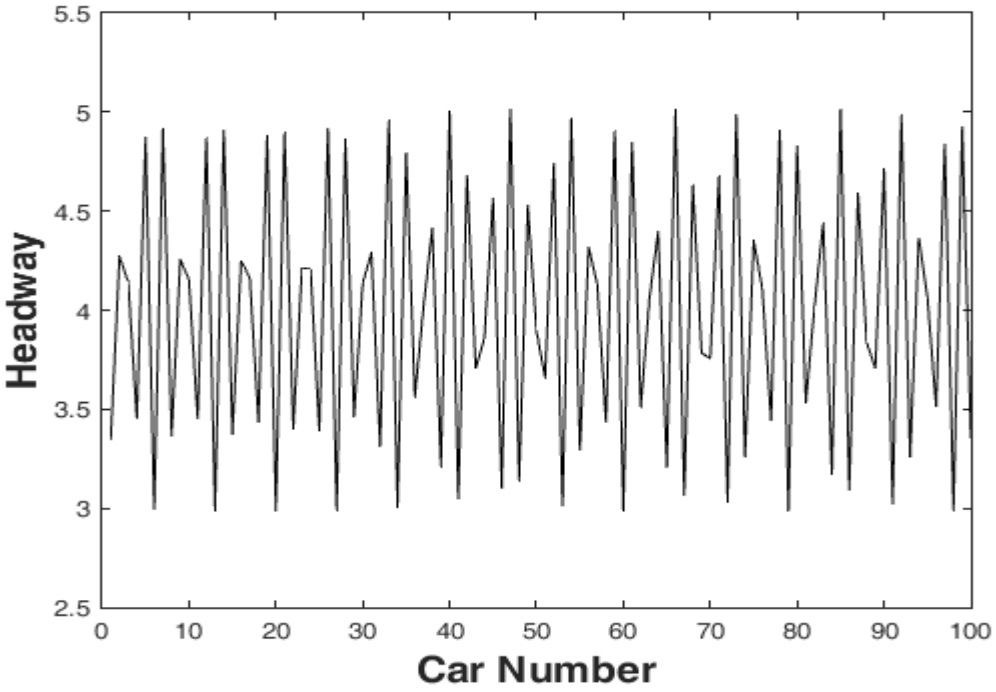

Fig. 3(d): "Headway profiles at t =10000s, the figure corresponding to $\lambda = 0$ and $p = 0.3$"

Figures 4(a)-4(d) represent the "spatiotemporal evolution of the headway" after t = 10000s for distinct values of p when $\lambda = 0.3$. For $p = 0$, we are in stable region, therefore, the initial perturbation dies out. As we increase the value of p from 0.1 to 0.3 shown in figures 4(b)-4(d), the initial uniform disturbance changes into "kink-antikink density wave," which are the solution of mKdV equation. These density waves propagate in backward direction with time as happen in real life traffic.

We can observe that the amplitude of density waves rises with an increase in the value of p from figures 5(a)-5(d), which shows that the region of traffic congestion grows with increase in the value of p.

The "spatiotemporal evolution of the headway" and "Headway profile" are shown in figures 6 and 7, respectively, for distinct values of p when $\lambda = 0.5$. Similar kinds of affect have been found for this case also.

From these figures, we observed that the quantity of stop and go wave rises as the value of p increases which implies that the traffic jam rises with increase in the value of p.

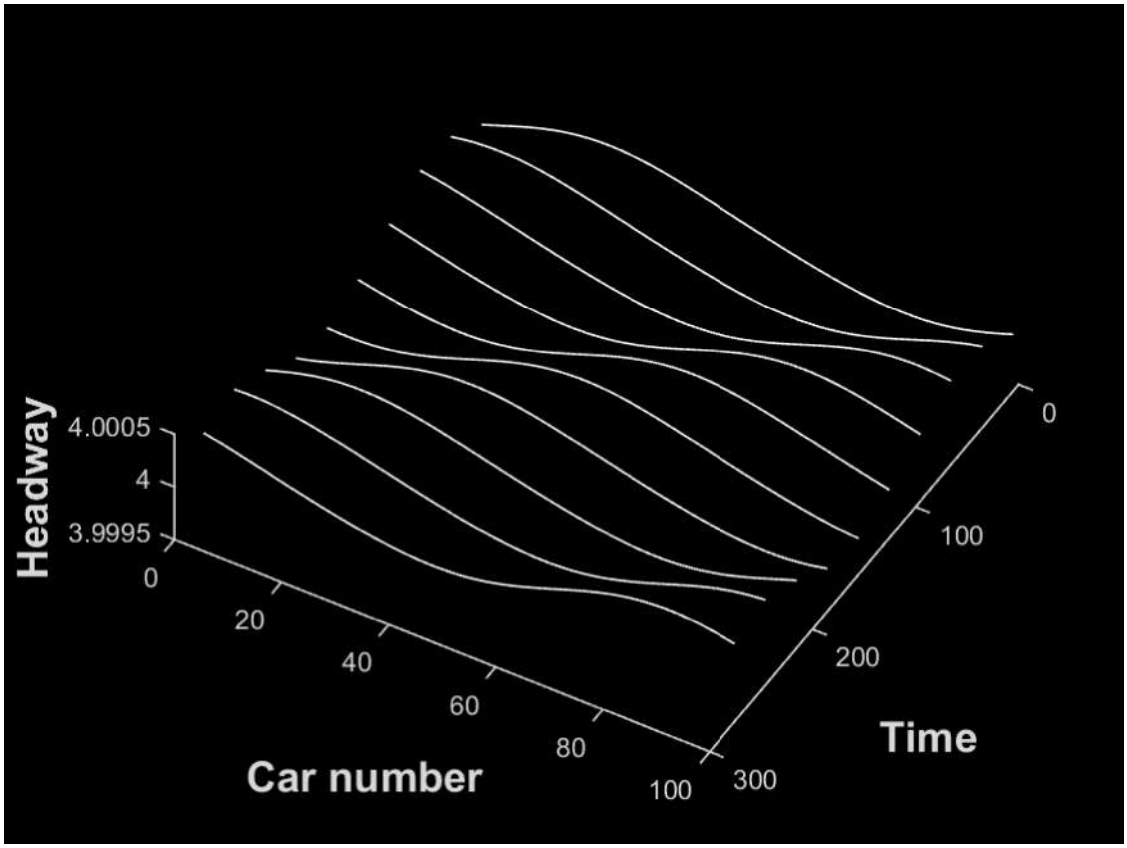

Fig. 4(a): "Headway evolution in space and time after t = 10000s for λ = 0.3 and p = 0"

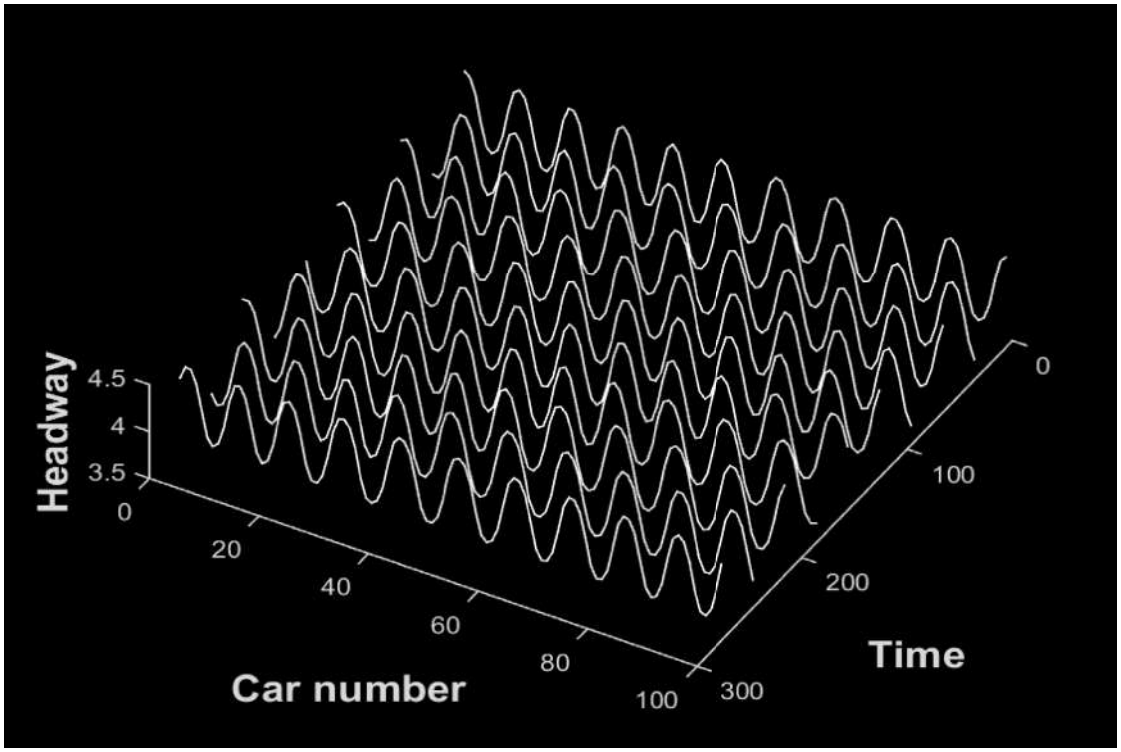

Fig. 4(b): "Headway evolution in space and time after t = 10000s for λ = 0.3 and p = 0.1"

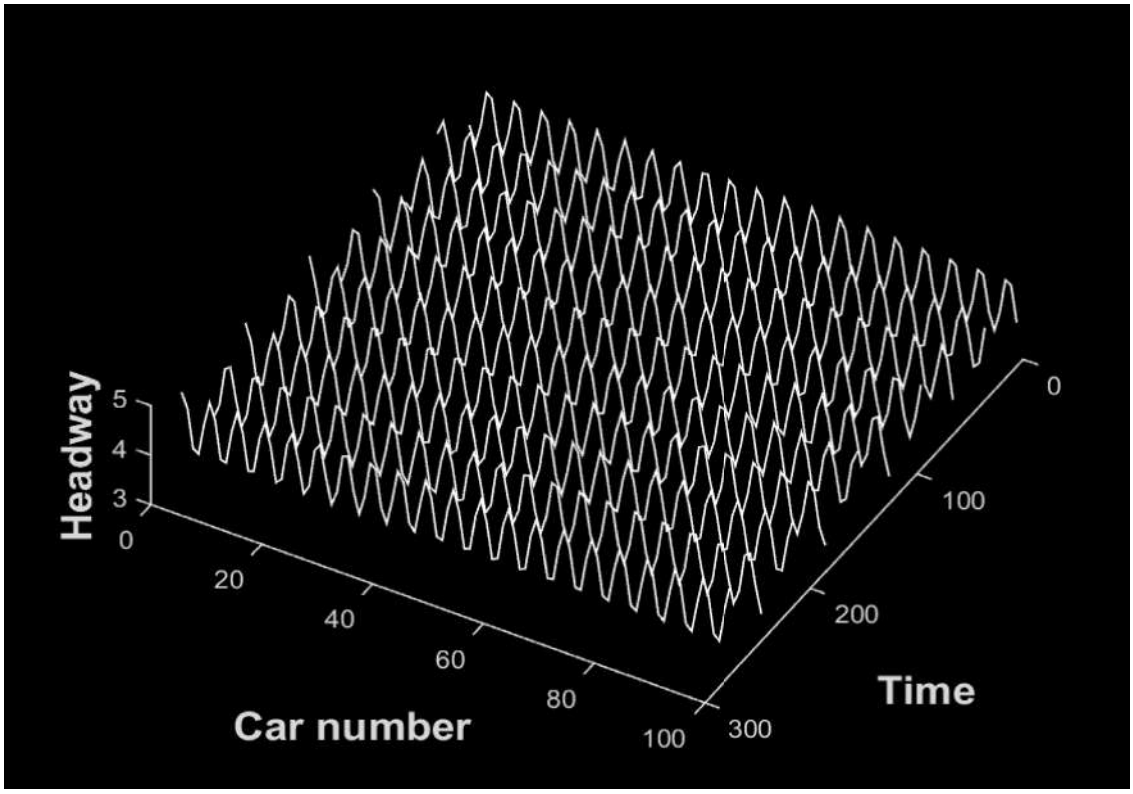

Fig. 4(c): "Headway evolution in space and time after t = 10000s for λ = 0.3 and p = 0.2"

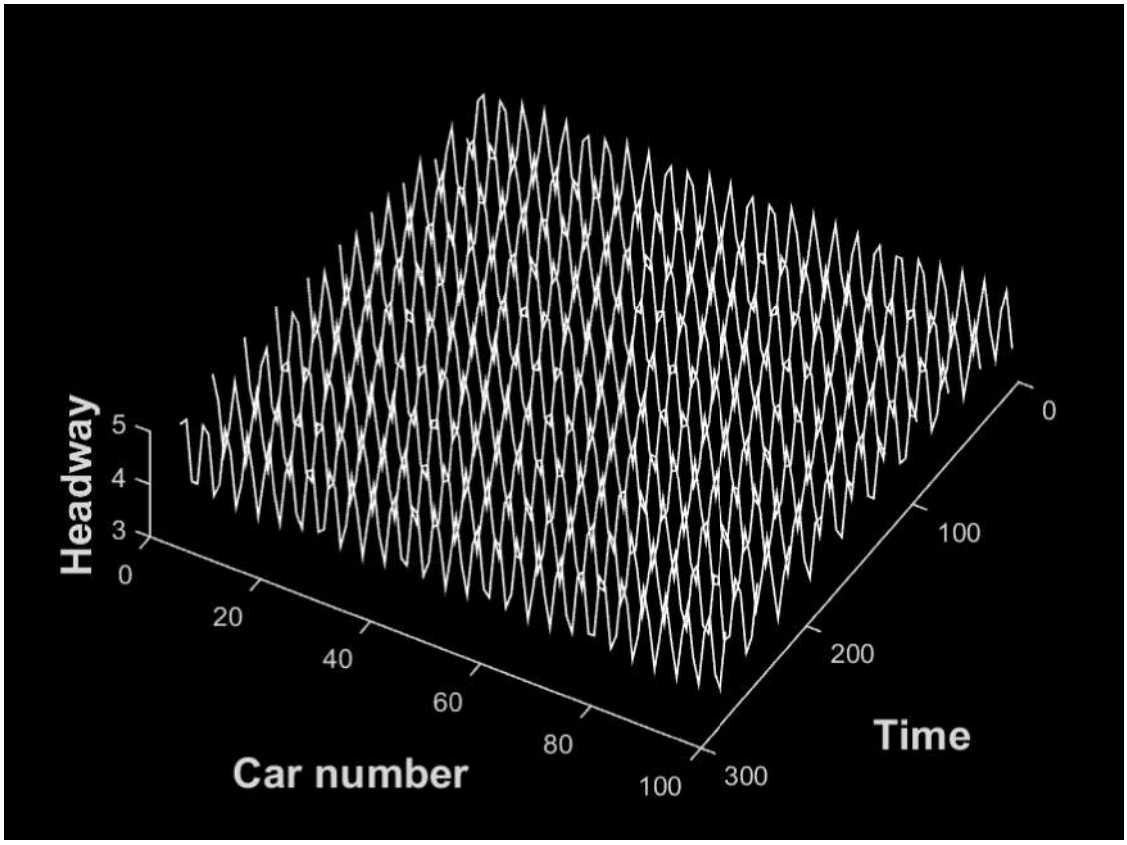

Fig. 4(d): "Headway evolution in space and time after t = 10000s for λ = 0.3 and p = 0.3"

Again from Figures 3(d), 5(d) and 7(d), it can be easily seen that the number of stop and go wave in Figure 3(d) is more than that of 7(d) which shows that traffic jam is more serious in 3(d) than that of 7(c) due to velocity difference.

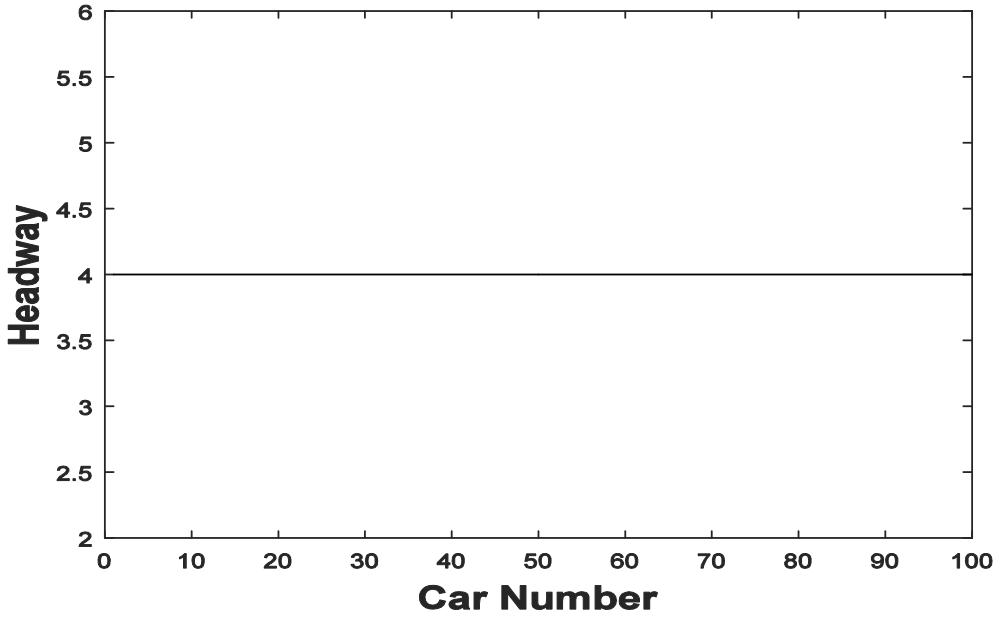

Fig. 5(a): "Headway profiles at t =10000s, the figure corresponding to λ = 0.3 and p = 0"

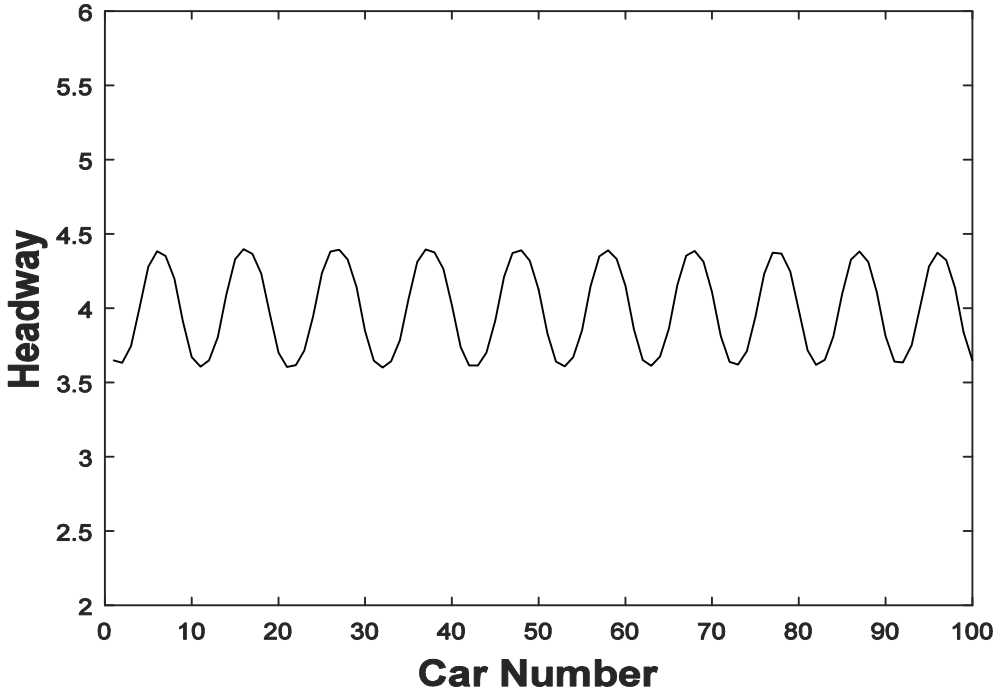

Fig. 5(b): "Headway profiles at t =10000s, the figure corresponding to λ = 0.3 and p = 0.1"

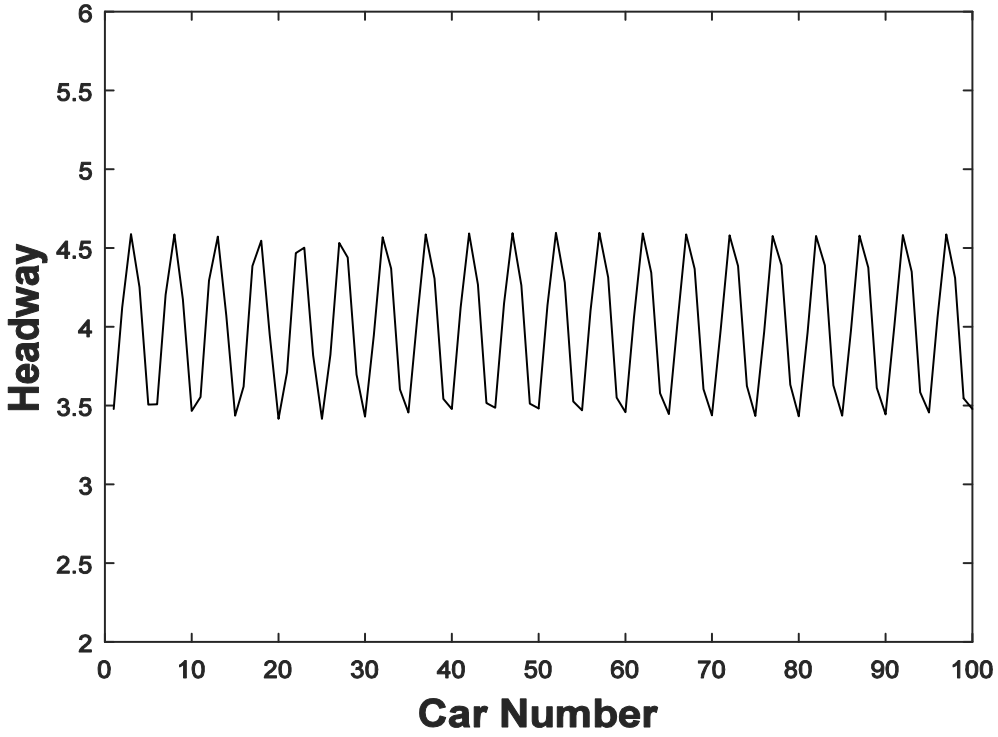

Fig. 5(c): " Headway profiles at t =10000s, the figure corresponding to λ = 0.3 and p = 0.2"

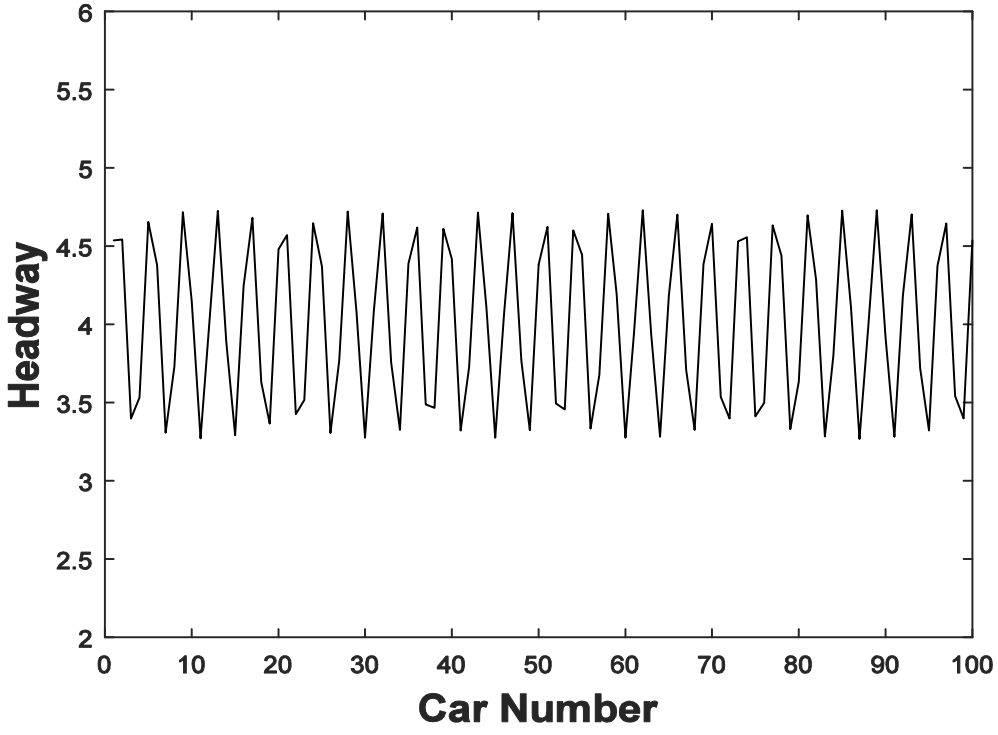

Fig. 5(d): "Headway profiles at t =10000s, the figure corresponding to λ = 0.3 and p = 0.3"

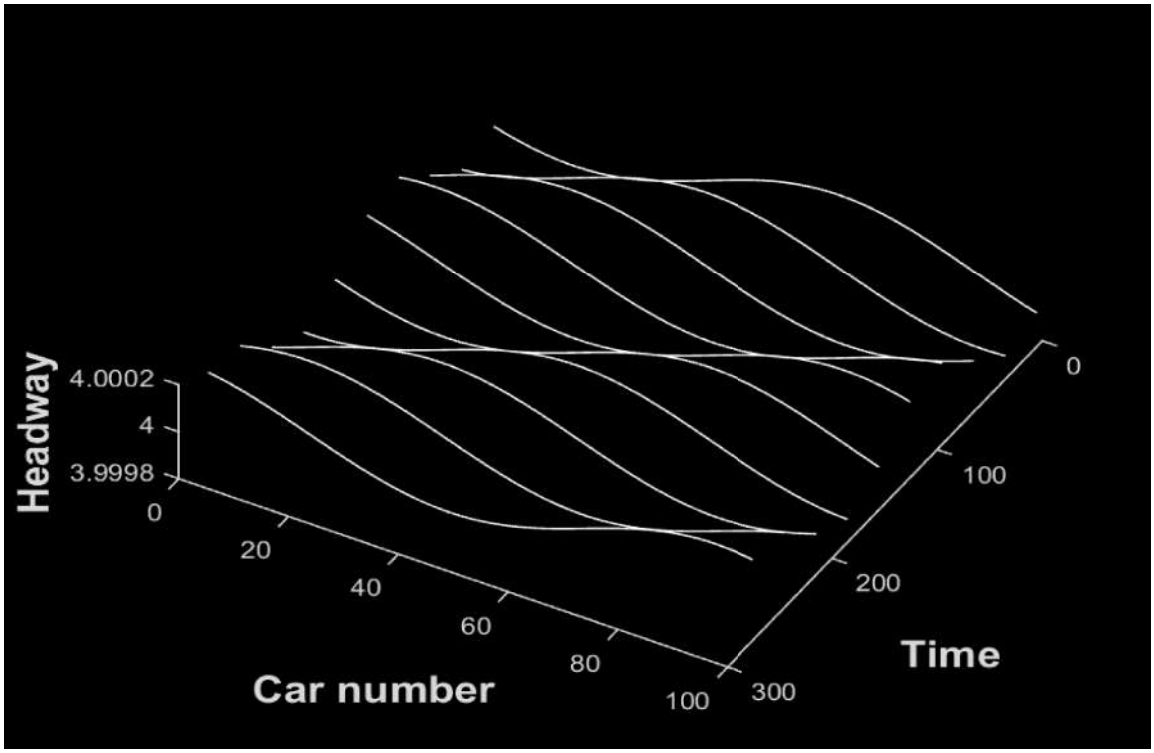

Fig. 6(a): "Headway evolution in space and time after t = 10000s for λ = 0.5 and p = 0"

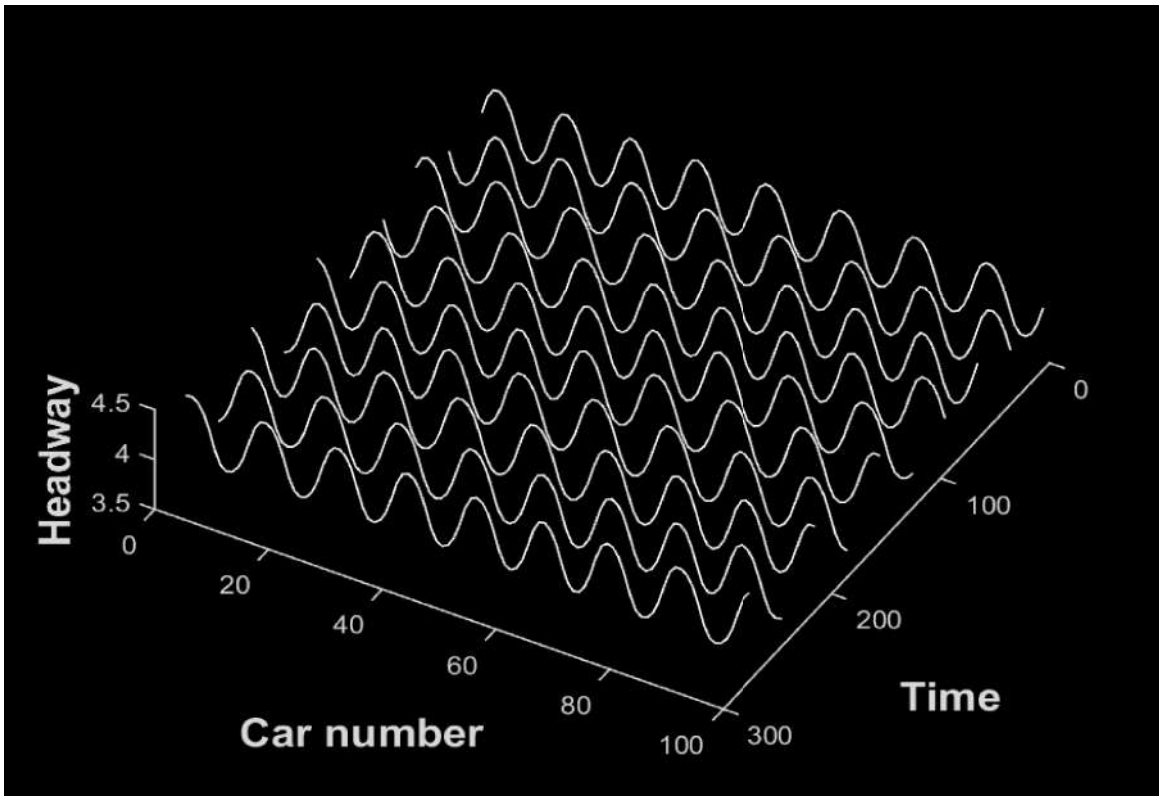

Fig. 6(b): "Headway evolution in space and time after t = 10000s for λ = 0.5 and p = 0.1"

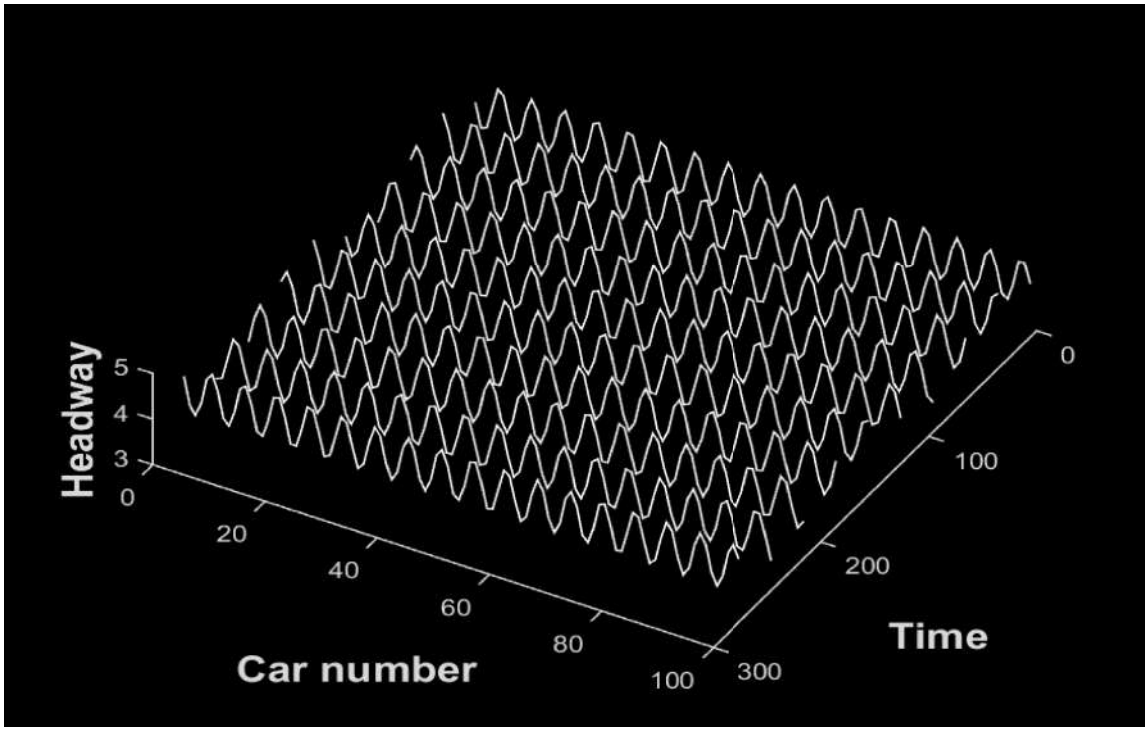

Fig. 6(c): "Headway evolution in space and time after t = 10000s for $\lambda = 0.5$ and $p = 0.2$"

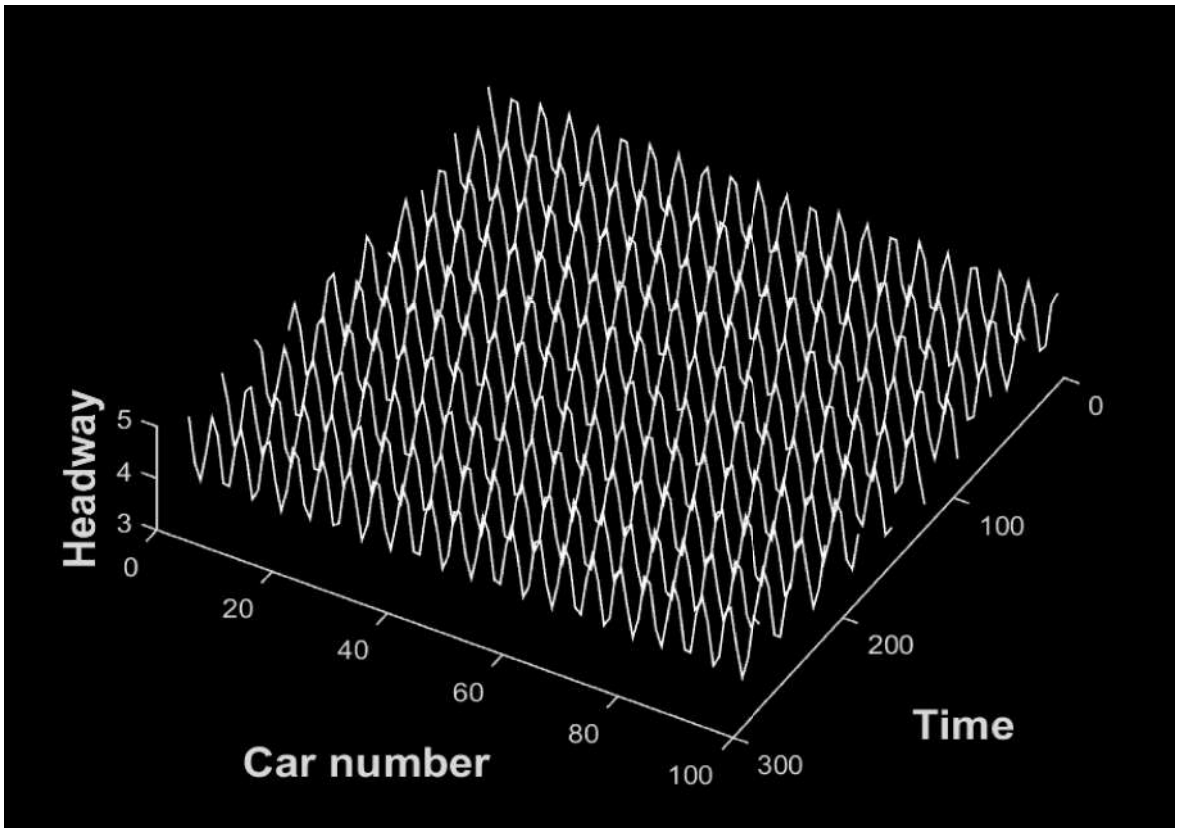

Fig. 6(d): "Headway evolution in space and time after t = 10000s for $\lambda = 0.5$ and $p = 0.3$"

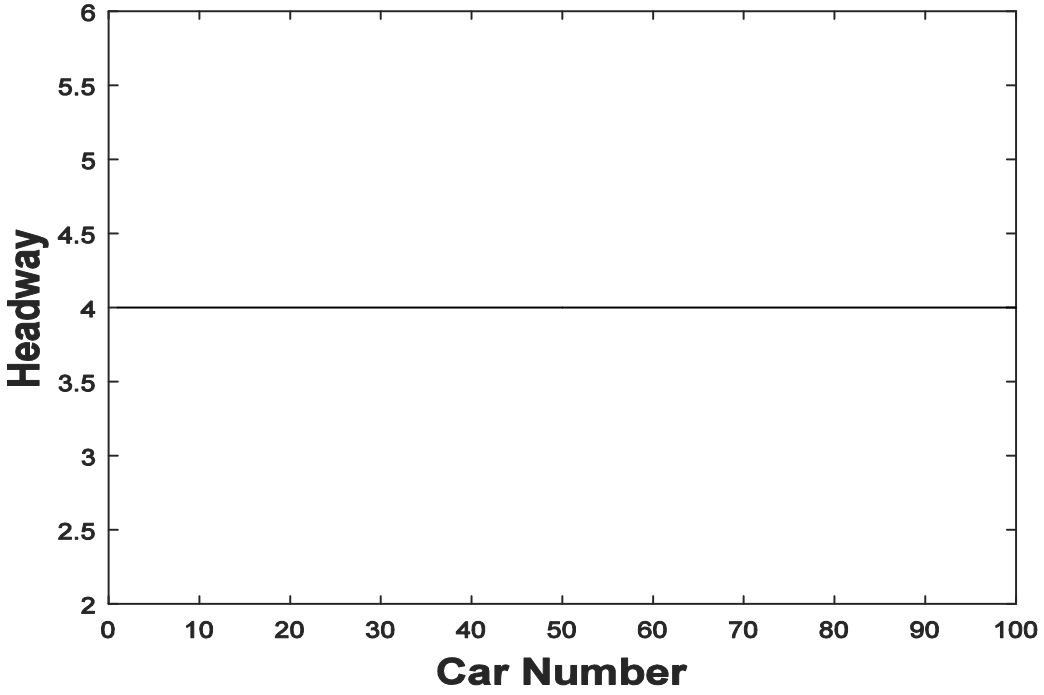

Fig. 7(a): "Headway profiles at t =10000s, the figure corresponding to λ = 0.5 and p = 0"

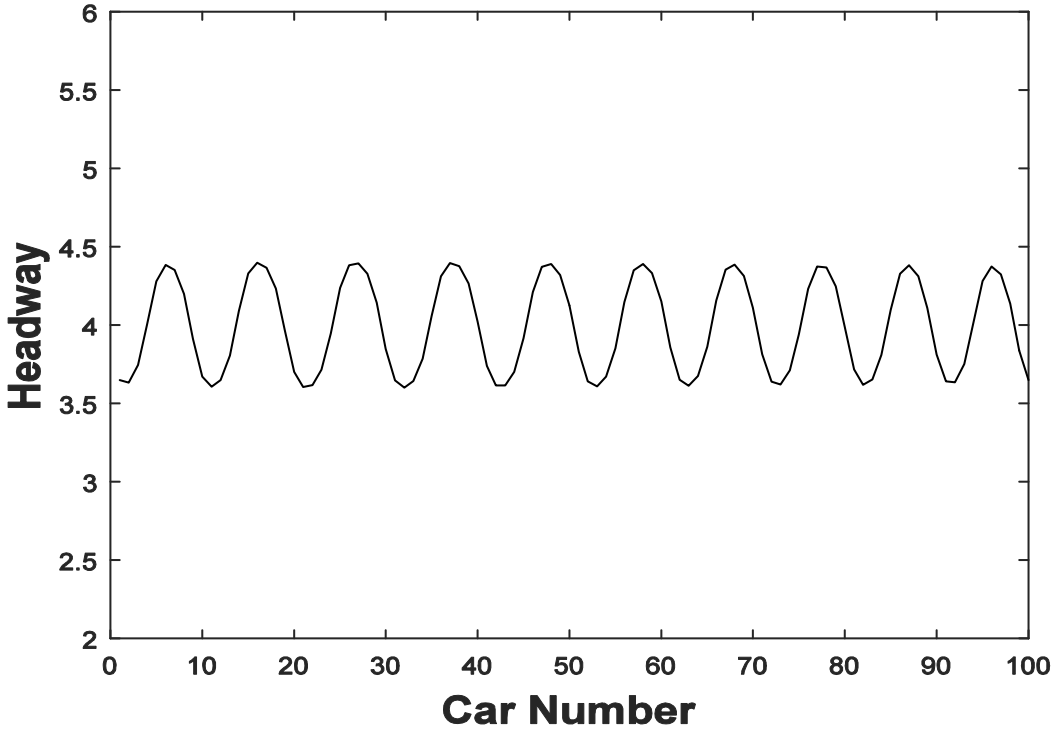

Fig. 7(b): "Headway profiles at t =10000s, the figure corresponding to λ = 0.5 and p = 0.1"

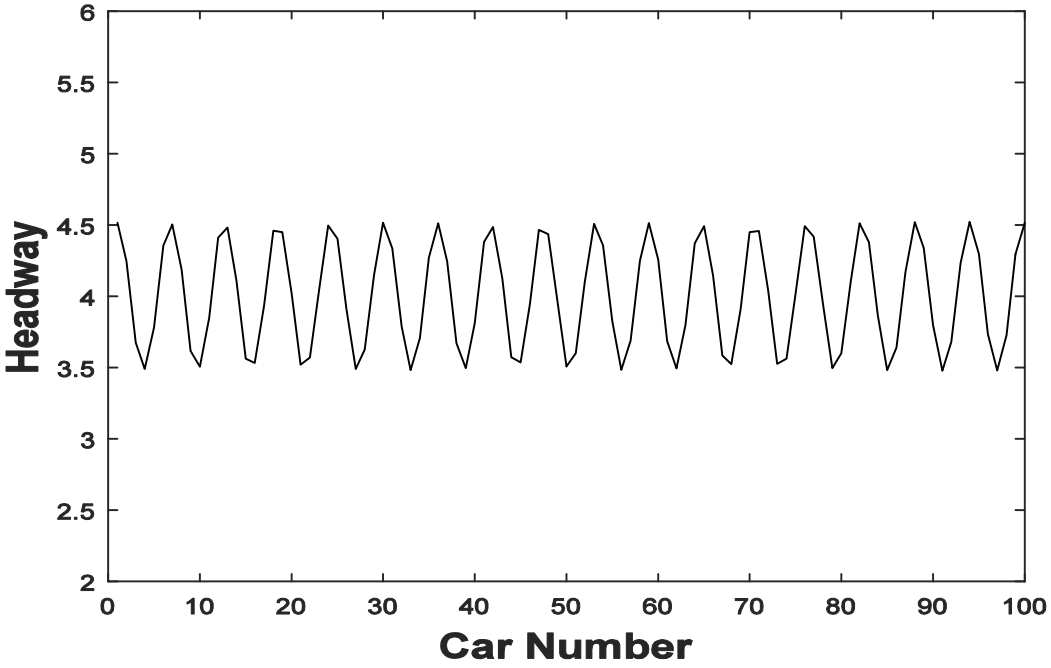

Fig. 7(c): "Headway profiles at t =10000s, the figure corresponding to $\lambda = 0.5$ and $p = 0.2$"

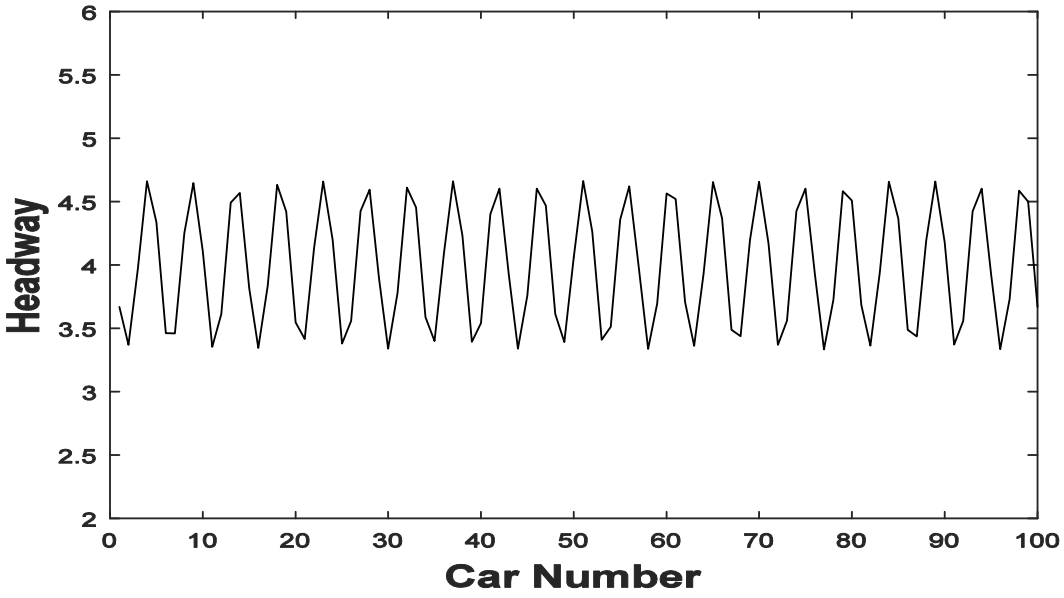

Fig. 7(d): "Headway profiles at t =10000s, the figure corresponding to $\lambda = 0.5$ and $p = 0.3$"

V CONCLUSION

In this chapter, an extended car-following model is presented by considering collective effect of velocity difference and driver's memory in the traffic flow. The stability criterion of the proposed model is found by linear stability analysis. The outcomes show that the stability

of traffic flow decreases with increase in the value of driver's memory time, also it is found that for a particular value of 'p', the stable region increase with increase in the value of 'λ'.

It should be noted that the traffic jam induced due to driver's memory can be overcome by considering the effect of velocity difference. In other words, we can say that if driver senses the information of leading vehicles in term of acceleration, then upto some level this information will be helpful in reducing the time consumed in congestion as well as in smooth driving. Therefore, it is obvious that both these factors play a significant role in traffic and these factors should be considered while modeling.

REFERENCES

1. Bando, M., Hasebe, K., Nakayama, A., Shibata, A. and Susiyama, Y. (1995). Dynamical model of traffic congestion and numerical simulation. Physical Review E, 51, 1035.
2. Jiang, R., Wu, Q.S. and Zhu, Z.J. (2001). Full velocity difference model for a car-following theory. Physical Review E, 64, 017101:1-017101:4.
3. Helbing, D. (1998). Generalized force model of traffic dynamics. Physical Review E, 58(1), 133-138.
4. Chakroborty, P. and Kikuchi, S. (1999). Evaluation of the General Motors based car-following models and a proposed fuzzy Inference model. Transportation Research Part C, 7, 209-235.
5. Tang, T.Q., Li, C.Y., Wu, Y.H. and Huang, H.J. (2011). Impact of the honk effect on the stability of traffic flow. Physica A: Statistical Mechanics and its Applications, 390(20), 3362-8.
6. Peng, G., Cai, X., Liu, C. and Cao, B. (2011). A new lattice model of traffic flow with the consideration of the honk effect. International Journal of Modern Physics C, 22(09), 967-76.
7. Tang, T.Q., Li, J.G., Huang, H.J. and Yang, X.B. (2014). A car-following model with real-time road conditions and numerical tests. Measurement, 48, 63-76.
8. Ge, H.X., Dai, S.Q., Dong, L.Y. and Xue, Y. (2004). Stabilization effect of traffic flow in an extended car-following model based on an intelligent transportation system application. Physical Review E, 70, 066134.
9. Gamel, S.A., Saleh A.I. and Ali H.A. (2021). Machine learning based traffic management technique for intelligent communication and computer science, vol. 1, pp. 9-18.
10. Shladover, S.E., Su, D. and Lu, X.Y. (2012). Impacts of cooperative adaptive cruise control on freeway traffic flow. Transportation Research Record, 2324(1), 63-70.

11. Zheng, L., Tian, J.C., Sun, D.H. and Liu, W.N. (2012). A new car-following model with consideration of anticipation driving behaviour. Nonlinear Dynamics, 70(2), 1205-1211.
12. Lighthill, M.J. and Whitham, G.B. (1955). On kinematic waves. ii. a theory of traffic flow on long crowded roads. Proceedings of the Royal Society of London. Series A, Mathematical and Physical Sciences, 229(1178):317-339.
13. Zhang, H.M. (2003). A macro model by incorporating the effect of driver's memory. Transportation Research B, 37, 27.
14. Peng, G.H., Nie, F.Y., Cao, B.F. and Liu, C.Q. (2012). A driver's memory lattice model of traffic flow and its numerical simulation. Nonlinear Dynamic, 67, 1811-1815.
15. Cao, B.G. (2015). A new car-following model considering driver's sensory memory. Physica A: Statistical Mechanics and its Application, 427, 218-25.